

Classical Limit for Scalar Fields at High Temperature

W. Buchmüller and A. Jakovác

Deutsches Elektronen-Synchrotron DESY, 22603 Hamburg, Germany

Abstract

We study real-time correlation functions in scalar quantum field theories at temperature $T = 1/\beta$. We show that the behaviour of soft, long wave length modes is determined by classical statistical field theory. The loss of quantum coherence is due to interactions with the soft modes of the thermal bath. The soft modes are separated from the hard modes by an infrared cutoff $\Lambda \ll 1/(\hbar\beta)$. Integrating out the hard modes yields an effective theory for the soft modes. The infrared cutoff Λ controls corrections to the classical limit which are $\mathcal{O}(\hbar\beta\Lambda)$. As an application, the plasmon damping rate is calculated.

1 Introduction

The properties of quantum field theories at high temperature are important in order to understand the behaviour of matter under extreme conditions, as they occur in astrophysics and cosmology. Static quantities at high temperature characterize the thermodynamics of the system, in particular the equation of state. Time-dependent quantities are relevant for the study of non-equilibrium processes, such as the generation of a cosmological baryon asymmetry.

Consider the partition function for a scalar field theory at temperature $T = 1/\beta$,

$$Z = \int_{\beta} \mathcal{D}\phi e^{-\frac{1}{\hbar} \int_0^{\hbar\beta} d\tau \int d^3x \mathcal{L}(\phi)} , \quad (1)$$

where the functional integration is over periodic fields, $\phi(\mathbf{x}, \hbar\beta) = \phi(\mathbf{x}, 0)$. Formally, the limit $T \rightarrow \infty$ is closely related to the limit $\hbar \rightarrow 0$. This suggests that the high temperature behaviour of bosonic systems may be described by an effective classical field theory. For static quantities this reasoning leads to the dimensional reduction program which has been successfully applied to the electroweak phase transition in recent years [1]. It has also been suggested that the classical theory can be used to compute real-time correlation functions at high temperature [2]. This is of particular interest for sphaleron processes in the electroweak theory where, however, results for the transition rate are still controversial [3, 4].

Scalar field theories are much simpler than gauge theories and therefore a useful starting point to study real-time processes at high temperature [5]. This concerns the problem of ultraviolet divergencies [6] as well as the question of quantum corrections to the classical limit [7]. In classical ϕ^4 -theory one studies the classical correlation functions

$$\langle \phi(\mathbf{x}_1, t_1) \dots \phi(\mathbf{x}_2, t_2) \rangle_{cl} = \frac{1}{Z} \int \mathcal{D}\pi \mathcal{D}\phi e^{-\beta H(\pi, \phi)} \phi(\mathbf{x}_1, t_1) \dots \phi(\mathbf{x}_2, t_2) , \quad (2)$$

where

$$H(\pi, \phi) = \int d^3x \left(\frac{1}{2} \pi^2 + \frac{1}{2} (\nabla \phi)^2 + \frac{1}{2} \mu^2 \phi^2 + \frac{1}{4!} \lambda \phi^4 \right) \quad (3)$$

is the classical Hamiltonian, and $\phi(\mathbf{x}, t)$ is the time-dependent field which is obtained by integrating the classical equations of motion from initial conditions $\phi(\mathbf{x}, t_i)$, $\pi(\mathbf{x}, t_i)$ over which then a thermal average is performed. From

the quantum thermal two-point function one obtains the plasmon damping rate [8]. As shown by Aarts and Smit [9], the damping rate is determined by the classical theory to leading order in the coupling λ . This result is most easily obtained from the retarded Green function, and it turns out that the whole imaginary part of the self-energy is given by the classical theory in the high-temperature limit [10]. The classical limit for scalar field theories has been further discussed in [11, 12].

The quantity $\hbar\beta$ carries dimension. Hence, the question arises which dimensionless quantity controls the classical limit. As is well known, the spectral energy density of a relativistic Bose gas, i.e., Planck's formula,

$$de = \frac{1}{\pi^2} \frac{\hbar\omega^3}{e^{\hbar\beta\omega} - 1} d\omega, \quad (4)$$

turns into the classical Rayleigh-Jeans formula

$$de = \frac{1}{\pi^2} T\omega^2 d\omega \quad (5)$$

for small frequencies,

$$\hbar\beta\omega \ll 1 \quad . \quad (6)$$

Hence, the classical limit is obtained for low frequency, long wave length modes. For high frequency modes there is no classical limit.

We conclude that a consistent definition of the classical limit requires the introduction of an infrared cutoff $\Lambda \ll 1/(\hbar\beta)$ which separates 'soft' modes with $\omega < \Lambda$ from 'hard' modes with $\omega > \Lambda$. The effective theory for the soft modes, where the hard modes have been integrated out, can be approximated by a classical theory. For massive theories one has $m < \hbar\omega < \hbar\Lambda$. Since at finite temperature a plasmon mass $m^2 \sim \hbar\lambda T^2$ is generated, the condition (6) implies $\hbar\lambda \ll 1$. Hence, a classical limit can only be obtained in the case of weak coupling.

In the following sections we shall discuss the connection between the finite-temperature quantum theory and the classical theory in detail. In sect. 2 we construct an effective theory for the low frequency modes. This is similar in spirit to the construction of an effective average action [14], and in particular to the Wilson renormalization group approach for thermal modes [15]. Sects. 3 and 4 deal with the infrared approximation which yields the classical limit up to corrections $\mathcal{O}(\hbar\beta\Lambda)$ and quantum corrections. As an application, we discuss the evaluation of the plasmon damping rate in sect. 5, and sect. 6 summarizes the main results. In the following we set $\hbar = 1$.

2 Low energy effective theory

The basic quantities of finite-temperature field theory are the thermal averages of time-ordered products of field operators,

$$\langle T\hat{\Phi}(x_1)\dots\hat{\Phi}(x_n)\rangle = \frac{1}{Z} \text{Tr} \left(e^{-\beta\hat{H}} T\hat{\Phi}(x_1)\dots\hat{\Phi}(x_n) \right) , \quad (7)$$

which can be obtained by differentiation from the functional

$$Z[j] = \text{Tr} \left(e^{-\beta\hat{H}} T_c e^{i\int_c dx j\hat{\Phi}} \right) . \quad (8)$$

Here T_c denotes ordering along an appropriately chosen path C in the complex time plane [16], and $\int_c dx j\hat{\Phi} \equiv \int_c dt \int d^3x j(\mathbf{x}, t)\hat{\Phi}(\mathbf{x}, t)$.

The dynamics of modes with energies ω below the temperature T is strongly affected by the thermal bath. In order to derive a low energy effective action for these modes one has to integrate out hard thermal modes. In the following we shall perform the part of the trace in Eq. (7) which involves large momentum modes. This procedure is similar to the Wilson renormalization group approach for thermal modes [15].

A convenient basis for the evaluation of the trace is provided by the coherent states of Bargmann and Fock (cf. [17]). They are constructed in terms of creation operators related to the field operator at some fixed time t_i ,

$$|\eta\rangle = N e^{\int_k \eta_{\mathbf{k}} a_{\mathbf{k}}^\dagger} |0\rangle , \quad (9)$$

where N is a normalization factor and

$$\int_{\mathbf{k}} = \int \frac{d^3k}{(2\pi)^3 2\omega_{\mathbf{k}}} . \quad (10)$$

The coherent states are eigenstates of annihilation operators,

$$a_{\mathbf{k}} |\eta\rangle = \eta_{\mathbf{k}} |\eta\rangle . \quad (11)$$

In the following we shall also use coherent states restricted to soft modes,

$$|\eta_\Lambda\rangle = N_\Lambda e^{\int_{|\mathbf{k}|<\Lambda} \eta_{\mathbf{k}} a_{\mathbf{k}}^\dagger} |0\rangle , \quad (12)$$

As discussed in the introduction, hard modes are defined by $\omega_{\mathbf{k}} > \Lambda$, where the separaton scale Λ has to be chosen in the range $m < \Lambda \ll \beta^{-1}$.

We can now split the trace which gives the functional $Z[j]$ into soft and hard modes,

$$Z[j] = \int_{\omega < \Lambda} \mathcal{D}\eta \mathcal{D}\eta^* Z_\Lambda[j] \quad , \quad (13)$$

where

$$\begin{aligned} Z_\Lambda[j] &= \int_{\omega > \Lambda} \mathcal{D}\eta \mathcal{D}\eta^* \langle \eta | e^{-\frac{1}{2}\beta\hat{H}} e^{i\int_c dx j \hat{\Phi}} e^{-\frac{1}{2}\beta\hat{H}} | \eta \rangle \\ &\equiv \text{Tr}_\Lambda \left(e^{-\frac{1}{2}\beta\hat{H}} e^{i\int_c dx j \hat{\Phi}} e^{-\frac{1}{2}\beta\hat{H}} \right) \quad , \end{aligned} \quad (14)$$

and $\mathcal{D}\eta \mathcal{D}\eta^* \propto \prod_{\mathbf{k}} d\eta_{\mathbf{k}} d\eta_{\mathbf{k}}^*$. The dependence of $Z_\Lambda[j]$ on the soft modes $\eta_{\mathbf{k}}$, $\omega_{\mathbf{k}} < \Lambda$, will be discussed in detail below. Note, that we have written the trace in a symmetric form in order to maintain the reality of expectation values of hermitian operators.

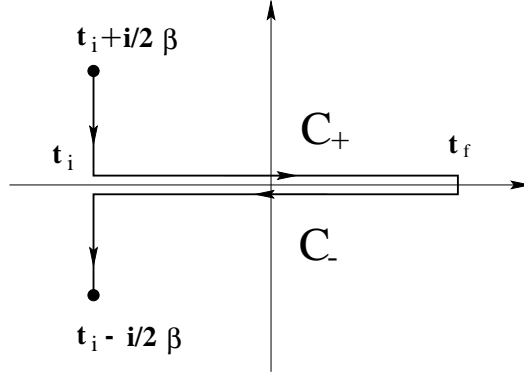


Figure 1: *Keldysh-type contour for real-time correlation functions*

The integral over the hard thermal modes yielding the functional $Z_\Lambda[j]$ can be carried out in perturbation theory. Using the usual methods of real-time perturbation theory [16] one easily derives the identity

$$e^{-\frac{1}{2}\beta\hat{H}} \mathbb{T}_c e^{i\int_c dx j \hat{\Phi}} e^{-\frac{1}{2}\beta\hat{H}} = e^{i\int_c dx \mathcal{L}_I(\frac{1}{i}\frac{\delta}{\delta j})} e^{-\frac{1}{2}\beta\hat{H}_0} \mathbb{T}_c e^{i\int_c dx j \hat{\Phi}_0} e^{-\frac{1}{2}\beta\hat{H}_0} \quad , \quad (15)$$

where the subscript 0 refers to free fields which are related to interacting fields by a unitary transformation. C is the Keldysh-type contour shown in

Fig. 1,

$$C : t_i + \frac{i}{2}\beta \rightarrow t_i \rightarrow t_f \rightarrow t_i \rightarrow t_i - \frac{i}{2}\beta. \quad (16)$$

From Eqs. (14) and (15) one reads off,

$$Z_\Lambda[j] = e^{i \int_c dx \mathcal{L}_I(\frac{1}{i} \frac{\delta}{\delta j})} Z_\Lambda^{(0)}[j], \quad (17)$$

where

$$Z_\Lambda^{(0)}[j] = \int_{\omega > \Lambda} \mathcal{D}\eta \mathcal{D}\eta^* \langle \eta | e^{-\frac{1}{2}\beta \hat{H}_0} \mathbb{T}_c e^{i \int_c dx j \hat{\Phi}_0} e^{-\frac{1}{2}\beta \hat{H}_0} | \eta \rangle. \quad (18)$$

In order to evaluate the integral over hard thermal modes we first express the time-ordered product in terms of a normal-ordered product,

$$\mathbb{T}_c e^{i \int_c dx j \hat{\Phi}_0} = e^{-\frac{1}{2} \int_c dx_1 dx_2 j(x_1) G_c(x_1, x_2) j(x_2)} : e^{i \int_c dx j \hat{\Phi}_0} : , \quad (19)$$

where G_c is the usual causal propagator [18],

$$\begin{aligned} G_c(x_1, x_2) &= \int_{\mathbf{k}} G_c(\mathbf{k}, t_1, t_2) e^{i\mathbf{k}(\mathbf{x}_1 - \mathbf{x}_2)} \\ &= \int_{\mathbf{k}} \left(\Theta(\tau_1 - \tau_2) e^{-i\omega_{\mathbf{k}}(t_1 - t_2)} \right. \\ &\quad \left. + \Theta(\tau_2 - \tau_1) e^{i\omega_{\mathbf{k}}(t_1 - t_2)} \right) e^{i\mathbf{k}(\mathbf{x}_1 - \mathbf{x}_2)}. \end{aligned} \quad (20)$$

Here τ , which parametrizes the contour C , is a real variable whereas $t(\tau)$ is in general complex.

For matrix elements of normal ordered products one easily proves the identity

$$\langle \eta_{\mathbf{k}} | e^{-\frac{1}{2}\beta \hat{H}_0} : f(a^\dagger, a) : e^{-\frac{1}{2}\beta \hat{H}_0} | \eta_{\mathbf{k}} \rangle = f(\eta_{\mathbf{k}}^* e^{-\frac{1}{2}\beta \omega_{\mathbf{k}}}, \eta_{\mathbf{k}} e^{-\frac{1}{2}\beta \omega_{\mathbf{k}}}) \langle \eta_{\mathbf{k}} | e^{-\beta \hat{H}_0} | \eta_{\mathbf{k}} \rangle. \quad (21)$$

This yields

$$\langle \eta | e^{-\frac{1}{2}\beta \hat{H}_0} : e^{i \int_c dx j \hat{\Phi}_0} : e^{-\frac{1}{2}\beta \hat{H}_0} | \eta \rangle = e^{i \int_c dx j \phi} \langle \eta | e^{-\beta \hat{H}_0} | \eta \rangle, \quad (22)$$

where the field ϕ is given by

$$\begin{aligned} \phi(\mathbf{x}, t) &= \frac{\langle \bar{\eta} | \hat{\phi}_0(\mathbf{x}, t) | \bar{\eta} \rangle}{\langle \bar{\eta} | \bar{\eta} \rangle} \\ &= \int_{\mathbf{k}} \left(\phi_{\mathbf{k}} \cos \omega_{\mathbf{k}}(t - t_i) + \frac{\pi_{\mathbf{k}}}{\omega_{\mathbf{k}}} \sin \omega_{\mathbf{k}}(t - t_i) \right) e^{i\mathbf{k}\mathbf{x}}, \end{aligned} \quad (23)$$

with

$$\phi_{\mathbf{k}} = e^{-\frac{1}{2}\beta\omega_{\mathbf{k}}} \left(\eta_{-\mathbf{k}}^* + \eta_{\mathbf{k}} \right) \quad , \quad \pi_{\mathbf{k}} = i\omega_{\mathbf{k}} e^{-\frac{1}{2}\beta\omega_{\mathbf{k}}} \left(\eta_{-\mathbf{k}}^* - \eta_{\mathbf{k}} \right) . \quad (24)$$

Here $|\bar{\eta}\rangle = \exp(-\frac{1}{2}\beta\hat{H}_0)|\eta\rangle$. A straightforward calculation yields for the matrix element of the free Hamiltonian,

$$\langle \eta | e^{-\beta\hat{H}_0} | \eta \rangle = \exp \left(-\frac{1}{4} \int_{\mathbf{k}} \frac{1}{n(\omega_{\mathbf{k}})} \left(|\phi_{\mathbf{k}}|^2 + \frac{1}{\omega_{\mathbf{k}}^2} |\pi_{\mathbf{k}}|^2 \right) \right) , \quad (25)$$

where $n(\omega)$ is the Bose-Einstein distribution function

$$n(\omega) = \frac{1}{e^{\beta\omega} - 1} . \quad (26)$$

The free functional $Z_{\Lambda}^{(0)}[j]$ can now be obtained from Eqs. (19), (22) and (25) by performing a Gaussian integration. The calculation gives the result

$$Z_{\Lambda}^{(0)}[j] = e^{-\beta H_{0,\Lambda}} e^{-\frac{1}{2} \int_c dx_1 dx_2 j(x_1) G_{\Lambda}(x_1, x_2) j(x_2)} e^{i \int_c dx j \phi_{\Lambda}} \quad , \quad (27)$$

where $H_{0,\Lambda}$ and ϕ_{Λ} are the free hamiltonian and the free field, respectively, restricted to soft modes,

$$\begin{aligned} e^{-\beta H_{0,\Lambda}} &= \langle \eta_{\Lambda} | e^{-\beta \hat{H}_0} | \eta_{\Lambda} \rangle , & (28) \\ \phi_{\Lambda}(x) &= \frac{\langle \bar{\eta}_{\Lambda} | \hat{\phi}_0(\mathbf{x}, t) | \bar{\eta}_{\Lambda} \rangle}{\langle \bar{\eta}_{\Lambda} | \bar{\eta}_{\Lambda} \rangle} \\ &= \int_{\mathbf{k}} \Theta(\omega - \Lambda) \left(\phi_{\mathbf{k}} \cos \omega_{\mathbf{k}}(t - t_i) + \frac{\pi_{\mathbf{k}}}{\omega_{\mathbf{k}}} \sin \omega_{\mathbf{k}}(t - t_i) \right) e^{i\mathbf{k}\mathbf{x}} , & (29) \end{aligned}$$

with $|\bar{\eta}_{\Lambda}\rangle = \exp(-\frac{1}{2}\beta\hat{H}_0)|\eta_{\Lambda}\rangle$. Integration over the hard modes leads to a corresponding thermal contribution to the propagator,

$$G_{\Lambda}(x_1, x_2) = G_c(x_1, x_2) + G_{T,\Lambda}(x_1 - x_2) \quad , \quad (30)$$

$$G_{T,\Lambda}(x_1 - x_2) = 2 \int_{\mathbf{k}} n_{\Lambda}(\omega_{\mathbf{k}}) \cos(\omega_{\mathbf{k}}(t_1 - t_2)) e^{i\mathbf{k}(\mathbf{x}_1 - \mathbf{x}_2)} , \quad (31)$$

where $n_{\Lambda}(\omega) = \Theta(\omega - \Lambda)n(\omega)$. From Eqs. (17) and (27) one obtains

$$\begin{aligned} Z_{\Lambda}[j] &= e^{-\beta H_{0,\Lambda}} e^{i \int_c dx \mathcal{L}_I(\frac{1}{i} \frac{\delta}{\delta j})} e^{i \int_c dx j \phi_{\Lambda}} e^{-\frac{1}{2} \int_c dx_1 dx_2 j(x_1) G_{\Lambda}(x_1, x_2) j(x_2)} \\ &= e^{-\beta H_{0,\Lambda}} e^{i \int_c dx j \phi_{\Lambda}} \tilde{Z}_{\Lambda}[j] , & (32) \end{aligned}$$

where

$$\tilde{Z}_\Lambda[j] = e^{i \int_c dx \mathcal{L}_I(\phi_\Lambda + \frac{1}{i} \frac{\delta}{\delta j})} e^{-\frac{1}{2} \int_c dx_1 dx_2 j(x_1) G_\Lambda(x_1, x_2) j(x_2)}. \quad (33)$$

Note, that Z_Λ and \tilde{Z}_Λ are functionals of j and ϕ_Λ , the soft modes, which play a role similar to a background field.

Using Eqs. (14) and (32) one can express the thermal Green functions in a compact form. Changing variables from η, η^* to ϕ, π the result reads

$$\begin{aligned} \langle \text{T}\hat{\Phi}(x_1) \dots \hat{\Phi}(x_n) \rangle &= \frac{1}{Z} \frac{1}{i^n} \frac{\delta}{\delta j(x_1)} \dots \frac{\delta}{\delta j(x_n)} Z[j] \Big|_{j=0} \\ &= \frac{1}{Z} \int_{\omega < \Lambda} \mathcal{D}\phi \mathcal{D}\pi e^{-\beta H_\Lambda} \langle \text{T}\hat{\Phi}(x_1) \dots \hat{\Phi}(x_n) \rangle_\Lambda \end{aligned} \quad (34)$$

where

$$H_\Lambda = H_{0,\Lambda} + H_{I,\Lambda} = -\frac{1}{\beta} \ln Z_\Lambda[0], \quad (35)$$

and

$$\langle \text{T}\hat{\Phi}(x_1) \dots \hat{\Phi}(x_n) \rangle_\Lambda = \frac{1}{Z_\Lambda} \frac{1}{i^n} \frac{\delta}{\delta j(x_1)} \dots \frac{\delta}{\delta j(x_n)} Z_\Lambda[j] \Big|_{j=0}. \quad (36)$$

From these expressions one can easily recover the usual real-time perturbation theory. The generating functional for the thermal Green functions is obtained by integrating $Z_\Lambda[j]$ over the soft modes. A Gaussian integration yields,

$$\int_{\omega < \Lambda} \mathcal{D}\eta \mathcal{D}\eta^* e^{-\beta H_{0,\Lambda}} e^{i \int_c dx j \phi_\Lambda} \propto e^{-\frac{1}{2} \int_c dx_1 dx_2 j(x_1) \bar{G}_{T,\Lambda}(x_1 - x_2) j(x_2)}, \quad (37)$$

where

$$\bar{G}_{T,\Lambda}(x) = 2 \int_{\mathbf{k}} \bar{n}_\Lambda(\omega_{\mathbf{k}}) \cos(\omega_{\mathbf{k}} t) e^{i \mathbf{k} \cdot \mathbf{x}}, \quad (38)$$

where $\bar{n}_\Lambda(\omega) = n(\omega) - n_\Lambda(\omega) = \Theta(\Lambda - \omega) n(\omega)$. Combining Eqs. (32) and (37) one obtains the familiar result

$$Z[j] = e^{i \int_c dx \mathcal{L}_I(\frac{1}{i} \frac{\delta}{\delta j})} e^{-\frac{1}{2} \int_c dx_1 dx_2 j(x_1) G(x_1, x_2) j(x_2)}, \quad (39)$$

where $G = G_\Lambda + \bar{G}_{T,\Lambda}$ is the usual thermal propagator [18]. The perturbation series for Green functions with infrared cutoff Λ is obtained from the perturbation series without cutoff by the following procedure: one substitutes the propagator $G(x - y)$ by $G_\Lambda(x - y)$, and one adds contributions which are obtained by replacing a propagator $G(x - y)$ by the product of background fields $\phi_\Lambda(x) \phi_\Lambda(y)$.

3 Infrared approximation

So far we have only reorganized the perturbative expansion, without making any approximation. In the resulting low energy effective theory, however, we have a small parameter, $\beta\Lambda \ll 1$, where Λ is the cutoff which distinguishes between soft and hard modes. As discussed in the introduction, in an expansion with respect to $\beta\Lambda$ the leading term should correspond to the classical limit. We shall refer to the leading term as the infrared (IR) approximation since, as we shall see, further approximations are necessary in order to obtain the classical limit.

Consider the thermal Green functions with IR cutoff Λ . From Eq. (32) one obtains

$$\frac{1}{i} \frac{\delta}{\delta j(x)} Z_\Lambda[j] = e^{-\beta H_{0,\Lambda}} e^{i \int_c dx j \phi_\Lambda} \left(\phi_\Lambda(x) + \frac{1}{i} \frac{\delta}{\delta j(x)} \right) \tilde{Z}_\Lambda[j] \quad , \quad (40)$$

and therefore

$$\begin{aligned} \langle T \hat{\Phi}(x_1) \dots \hat{\Phi}(x_n) \rangle_\Lambda &= \frac{1}{\tilde{Z}_\Lambda} \left(\phi_\Lambda(x_1) + \frac{1}{i} \frac{\delta}{\delta j(x_1)} \right) \dots \\ &\quad \left(\phi_\Lambda(x_n) + \frac{1}{i} \frac{\delta}{\delta j(x_n)} \right) \tilde{Z}_\Lambda[j] \Big|_{j=0} . \end{aligned} \quad (41)$$

The right-hand side of the equation is the sum of products of $n - m$ fields ϕ_Λ ($0 \leq m \leq n$) and m -point functions

$$\tilde{\tau}(y_1, \dots, y_m) = \frac{1}{\tilde{Z}_\Lambda} \frac{1}{i^m} \frac{\delta}{\delta j(y_1)} \dots \frac{\delta}{\delta j(y_m)} \tilde{Z}_\Lambda[j] \Big|_{j=0} . \quad (42)$$

The $\tilde{\tau}$ -functions can be computed as usual in perturbation theory. According to Eq. (32), $\phi_\Lambda(x)$ occurs as a background field which leads to additional vertices (cf. Fig. 2). The $\tilde{\tau}$ -functions can be decomposed into disconnected and connected parts (cf., e.g., [19]),

$$\begin{aligned} \tilde{\tau}(y_1, \dots, y_m) &= \tilde{\tau}(y_1) \dots \tilde{\tau}(y_m) \\ &\quad + \tilde{\tau}(y_1, y_2)_c \tilde{\tau}(y_3) \dots \tilde{\tau}(y_m) + \text{permutations} \\ &\quad + \dots \\ &\quad + \tilde{\tau}(y_1, \dots, y_m)_c . \end{aligned} \quad (43)$$

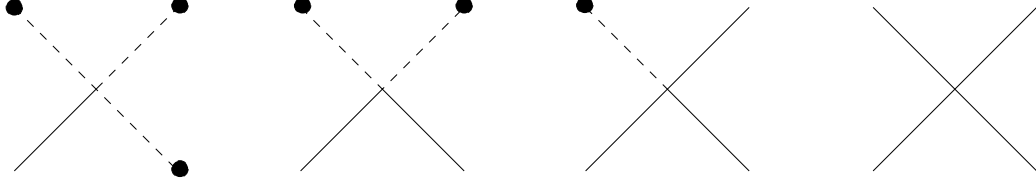


Figure 2: Vertices in the presence of the background field ϕ_Λ

For the tadpole one obviously has (cf. (40)),

$$\tilde{\tau}(y) = \langle \hat{\Phi}(y) \rangle_\Lambda - \phi_\Lambda(y). \quad (44)$$

From Eqs. (41)-(44) one obtains

$$\langle T\hat{\Phi}(x_1) \dots \hat{\Phi}(x_n) \rangle_\Lambda = \langle \hat{\Phi}(x_1) \rangle_\Lambda \dots \langle \hat{\Phi}(x_n) \rangle_\Lambda + \text{PC}, \quad (45)$$

where PC denotes partially connected contributions which contain connected m -point functions.

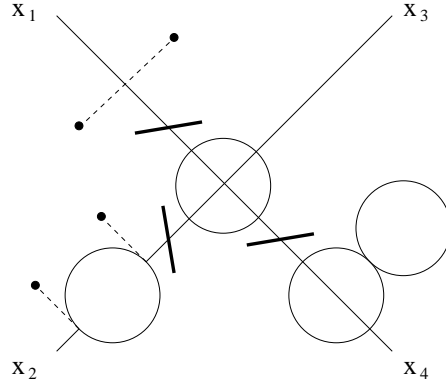


Figure 3: Contribution to $\tilde{\tau}(x_1, \dots, x_4)_c$ with cuts indicated

Consider a particular contribution to PC with a connected m -point function $\tilde{\tau}(y_1, \dots, y_m)_c$ (cf. Fig. 3). Substituting for $m - 1$ lines

$$G_\Lambda(y - z) \rightarrow \phi_\Lambda(y)\phi_\Lambda(z) \quad (46)$$

yields a contribution to $\langle \hat{\Phi}(x_1) \rangle_\Lambda \dots \langle \hat{\Phi}(x_n) \rangle_\Lambda$ (cf. Fig. 4). Hence, for each contribution to PC there exists a corresponding term contained in the disconnected product $\langle \hat{\Phi}(x_1) \rangle_\Lambda \dots \langle \hat{\Phi}(x_n) \rangle_\Lambda$.

In order to obtain the complete thermal Green functions we still have to integrate over the soft modes. As discussed in the previous section, the integration $\int_{\omega < \Lambda} \mathcal{D}\phi \mathcal{D}\pi$ replaces products of background fields by the infrared propagator $\bar{G}_{T,\Lambda}$ (cf. Eq. (37)),

$$\phi_\Lambda(y)\phi_\Lambda(z) \rightarrow \int_{\omega < \Lambda} \bar{G}_{T,\Lambda}(\mathbf{k}, y_0 - z_0) e^{i\mathbf{k}(y-z)}. \quad (47)$$

For soft modes, with

$$\omega < \Lambda \ll T, \quad (48)$$

the propagators G_Λ and $\bar{G}_{T,\Lambda}$, which occur in the disconnected and connected contributions, respectively, satisfy the inequality,

$$G_\Lambda(\mathbf{k}, t) \sim \frac{1}{\omega_{\mathbf{k}}} < \beta\Lambda \frac{T}{\omega_{\mathbf{k}}^2} \sim \beta\Lambda \bar{G}_{T,\Lambda}(\mathbf{k}, t). \quad (49)$$

This implies that the dominant contribution to thermal Green functions is determined by the disconnected term $\langle \hat{\Phi}(x_1) \rangle_\Lambda \dots \langle \hat{\Phi}(x_n) \rangle_\Lambda$ for soft external momenta, i.e., $|\mathbf{x}_i - \mathbf{x}_j| > 1/\Lambda$. From Eqs. (34) and (45) one obtains in this case,

$$\langle \text{T}\hat{\Phi}(x_1) \dots \hat{\Phi}(x_n) \rangle = \frac{1}{Z} \int_{\omega < \Lambda} \mathcal{D}\phi \mathcal{D}\pi e^{-\beta H_\Lambda} \langle \hat{\Phi}(x_1) \rangle_\Lambda \dots \langle \hat{\Phi}(x_n) \rangle_\Lambda + \mathcal{O}(\beta\Lambda). \quad (50)$$

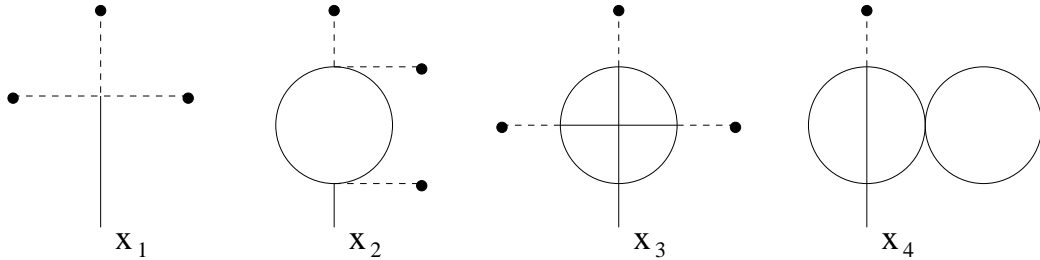


Figure 4: The tadpole diagrams corresponding to the cut components

This equation is the main result of this paper. It is similar to the ansatz of classical statistical field theory, as described in the introduction. There are, however, several differences with respect to the classical theory.

Consider first the hamiltonian H_Λ , as defined in Eqs. (35) and (36). The interaction part is, to leading order in the loop expansion,

$$H_{I,\Lambda} = - \int d^3x \mathcal{L}_I(\phi(\mathbf{x}, t_i)) + \mathcal{O}(\beta\Lambda) . \quad (51)$$

Higher order corrections can be calculated in perturbation theory and yield further deviations from the classical Hamiltonian. Further, as we shall see in the next section, also the initial conditions for the fields $\langle \hat{\Phi}(\mathbf{x}, t) \rangle_\Lambda$ and $\langle \hat{\Pi}(\mathbf{x}, t) \rangle_\Lambda = \langle \partial_t \hat{\Phi}(\mathbf{x}, t) \rangle_\Lambda$ are different from the integration variables in the functional integral (50).

Hence, except for the momentum cutoff, the integration over ϕ and π corresponds to an integral over all possible initial conditions. Eq. (50) differs from the naive classical limit by the presence of the momentum cutoff Λ , by quantum corrections to the classical hamiltonian and by the deviation of the time evolution of $\langle \hat{\Phi}(x) \rangle_\Lambda$ from the classical evolution.

It is very interesting that in the high-temperature limit the coherence of the quantum fields is lost to leading order in $\beta\Lambda$. In Eq. (50) the expectation value of the product of field operators has been replaced by the corresponding product of expectation values, and the time ordering has therefore lost its meaning. This is an effect of the thermal bath where the propagator of the soft modes is dominated by the thermal part $\bar{G}_{T,\Lambda}$.

4 Time evolution of expectation values

In order to understand the connection between the infrared approximation and the classical approximation one has to study the time evolution of field expectation values in the low energy effective theory. The time dependent field

$$\langle \hat{\Phi}(x) \rangle_\Lambda = \frac{1}{Z_\Lambda} \text{Tr}_\Lambda \left(e^{-\beta \hat{H}} \hat{\Phi}(x) \right) \quad (52)$$

can be evaluated in perturbation theory. From Eqs. (32) and (33) one reads off,

$$\langle \hat{\Phi}(x) \rangle_{\Lambda} = \left(\phi_{\Lambda}(x) + \frac{1}{i} \frac{\delta}{\delta j(x)} \right) e^{i \int_c dx \mathcal{L}_I(\phi_{\Lambda} + \frac{1}{i} \frac{\delta}{\delta j})} e^{-\frac{1}{2} \int_c dx_1 dx_2 j(x_1) G_{\Lambda}(x_1, x_2) j(x_2)} \Big|_{j=0}. \quad (53)$$

To be specific, consider a quartic self-interaction,

$$\mathcal{L}_I(\phi) = \frac{\lambda}{4!} \phi^4. \quad (54)$$

The corresponding Feynman diagrams contributing to $\langle \hat{\Phi}(x) \rangle_{\Lambda}$ are shown in Fig. 5 up to two loops.

The kinetic operator for a mode with momentum \mathbf{k} is

$$K_0(\mathbf{k}) = \frac{d^2}{d^2t} + \omega_{\mathbf{k}}^2. \quad (55)$$

From the definitions (29) and (30) one reads off that the background field ϕ_{Λ} and the propagator G_{Λ} satisfy the equations ($t_i < t < t_f$),

$$\begin{aligned} K_0(\mathbf{k})\phi_{\Lambda}(\mathbf{k}, t) &= 0, \\ K_0(\mathbf{k})G_{\Lambda}(\mathbf{k}, t) &= -i\delta(t). \end{aligned} \quad (56)$$

Furthermore, one easily obtains for the field $\langle \hat{\Phi}(x) \rangle_{\Lambda}$, up to terms $\mathcal{O}(\lambda^3)$ (cf. Fig. 5),

$$K_0 \langle \hat{\Phi} \rangle_{\Lambda} = -\frac{\lambda}{3!} \langle \hat{\Phi} \rangle_{\Lambda}^3 - (D_c + D_h + D_j) \langle \hat{\Phi} \rangle_{\Lambda} - \langle \hat{\Phi} \rangle_{\Lambda} D_i \langle \hat{\Phi} \rangle_{\Lambda}^2. \quad (57)$$

Here the D_n are non-local kernels which give the contributions of the corresponding 1PI diagrams in Fig. 5. Eq. (57) is similar to the classical equation of motion. The only difference is that the coupling constants m^2 and λ have been replaced by *non-local* kernels. Note also, that higher orders in the loop expansion will generate higher powers of $\langle \hat{\Phi} \rangle_{\Lambda}$ in Eq. (57).

Also important are the initial conditions which solutions of Eq. (57) have to satisfy. From Eq. (53) it is clear that

$$\langle \hat{\Phi}(\mathbf{x}, 0) \rangle_{\Lambda} \neq \phi_{\Lambda}(\mathbf{x}, 0). \quad (58)$$

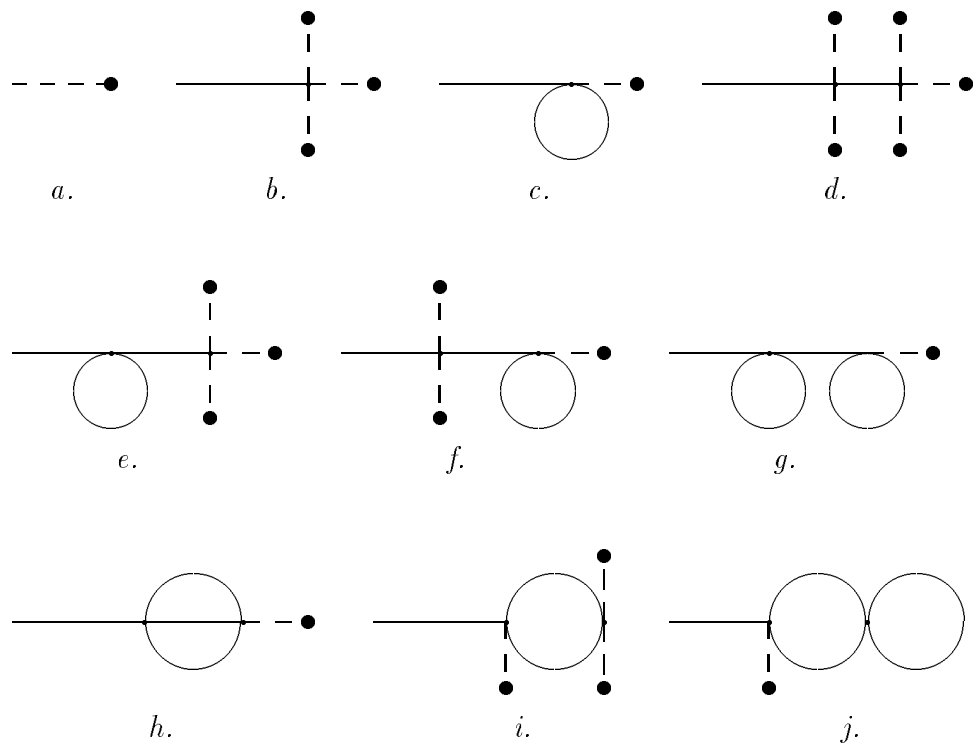


Figure 5: Contribution to $\langle \hat{\Phi}(x) \rangle_\Lambda$ up to two loops

Instead, one finds for the Fourier coefficients of both fields,

$$\begin{aligned}\langle \hat{\Phi}(\mathbf{k}, 0) \rangle_{\Lambda} &= \phi_{\mathbf{k}} + \mathcal{O}(\lambda\beta\Lambda) , \\ \langle \partial_t \hat{\Phi}(\mathbf{k}, t) \rangle_{\Lambda} \Big|_{t=0} &= \pi_{\mathbf{k}} + \mathcal{O}(\lambda\beta\Lambda) .\end{aligned}\quad (59)$$

Hence, the integration variables in the infrared approximation (50) agree with the initial conditions of the field $\langle \hat{\Phi}(x) \rangle_{\Lambda}$ only up to corrections $\mathcal{O}(\lambda\beta\Lambda)$.

Consider now the quantum corrections to the classical field equation. At one loop we have to consider the diagrams Figs. 5c and 5i. The first term is local and leads to an effective thermal mass,

$$m_{eff}^2 = m_B^2 + \frac{\lambda}{2} \int_{\mathbf{k}} G_{\Lambda}(\mathbf{k}, 0) = m_R^2 + \frac{\lambda}{24} T^2 \left(1 - \frac{6}{\pi^2} \beta\Lambda \right) = m_{\Lambda}(T)^2 . \quad (60)$$

Here m_B and m_R are the bare mass and the renormalized mass of the zero temperature 4D theory, respectively. The thermal mass $m_{\Lambda}(T)$ is well known from finite-temperature perturbation theory.

Diagram 5i yields the contribution

$$\langle \hat{\Phi}(x) \rangle_{\Lambda} D_i \langle \hat{\Phi} \rangle_{\Lambda}^2(x) = -i \frac{\lambda^2}{4} \langle \hat{\Phi}(x) \rangle_{\Lambda} \int_c dx' G_{\Lambda}(x, x')^2 \langle \hat{\Phi}(x') \rangle_{\Lambda}^2 , \quad (61)$$

where the contour integral can be carried out by means of the two-component formalism (cf. appendix). The divergent contribution is again renormalized as in the zero temperature 4D theory. The contributions 5b and 5i can be combined to an effective non-local coupling. A straightforward calculation yields the result (cf. appendix),

$$\lambda_{eff}(x - x') = \lambda(T) \delta(x - x') + \lambda_{nonloc}(x - x') , \quad (62)$$

where $\lambda(T)$ is the temperature dependent coupling familiar from dimensional reduction [21],

$$\lambda(T) = \lambda_R(\mu) \left(1 - \frac{1}{4\pi^2} \ln \frac{\mu}{T} \right) + \mathcal{O}(\beta\Lambda) , \quad (63)$$

and

$$\begin{aligned}
\lambda_{nonloc}(\mathbf{k}, t - t') &= \frac{3\lambda^2}{4} \int \frac{d^3\mathbf{q}}{(2\pi)^3} \frac{1}{\omega_{\mathbf{q}}\omega_{\mathbf{k}-\mathbf{q}}} \\
&\left[\frac{1 + n_{\Lambda}(\omega_{\mathbf{q}}) + n_{\Lambda}(\omega_{\mathbf{k}-\mathbf{q}})}{\omega_{\mathbf{q}} + \omega_{\mathbf{k}-\mathbf{q}}} \cos(\omega_{\mathbf{q}} + \omega_{\mathbf{k}-\mathbf{q}})(t - t') + \right. \\
&+ \left. \frac{n_{\Lambda}(\omega_{\mathbf{k}-\mathbf{q}}) - n_{\Lambda}(\omega_{\mathbf{q}})}{\omega_{\mathbf{q}} - \omega_{\mathbf{k}-\mathbf{q}}} \cos(\omega_{\mathbf{q}} - \omega_{\mathbf{k}-\mathbf{q}})(t - t') \right] \Theta(t - t') \frac{\partial}{\partial t'} \\
&+ \mathcal{O}(\beta\Lambda) . \tag{64}
\end{aligned}$$

To obtain this result we have performed a partial integration in t' and discarded the contribution at $t' = -\infty$ (cf. [20]). From the upper limit of integration $t' = t$ one obtains a contribution which is local in space up to corrections $\mathcal{O}(\beta\Lambda)$ [21]. The important infrared contribution to the non-local part of the coupling was previously found by Boyanovski et al. in a non-equilibrium context [20].

5 Retarded Green function

An interesting illustration of the classical limit is the calculation of the plasmon damping rate [9], which is most easily evaluated by considering the retarded Green function [10].

The retarded Green function of the low energy effective theory is given by

$$iD_{\Lambda}^R(x_1, x_2) = \frac{1}{Z} \text{Tr}_{\Lambda} \left(e^{-\beta\hat{H}} \left[\hat{\Phi}(x_1), \hat{\Phi}(x_2) \right] \right) \Theta(t_1 - t_2) . \tag{65}$$

It can be obtained from the time-ordered Green function by means of the following relations,

$$iD_{\Lambda}^R(x_1, x_2) = (D_{\Lambda}^>(x_1, x_2) - D_{\Lambda}^<(x_1, x_2)) \Theta(t_1 - t_2) , \tag{66}$$

and

$$\langle T\hat{\Phi}(x_1)\hat{\Phi}(x_2) \rangle_{\Lambda} = D_{\Lambda}^>(x_1, x_2) \Theta(t_1 - t_2) + D_{\Lambda}^<(x_1, x_2) \Theta(t_2 - t_1) . \tag{67}$$

As discussed in Sect. 3, the time-ordered Green function is the sum of a disconnected and a connected piece,

$$\langle T\hat{\Phi}(x_1)\hat{\Phi}(x_2) \rangle_{\Lambda} = \langle \hat{\Phi}(x_1) \rangle_{\Lambda} \langle \hat{\Phi}(x_2) \rangle_{\Lambda} + D_{\Lambda}^c(x_1, x_2) . \tag{68}$$

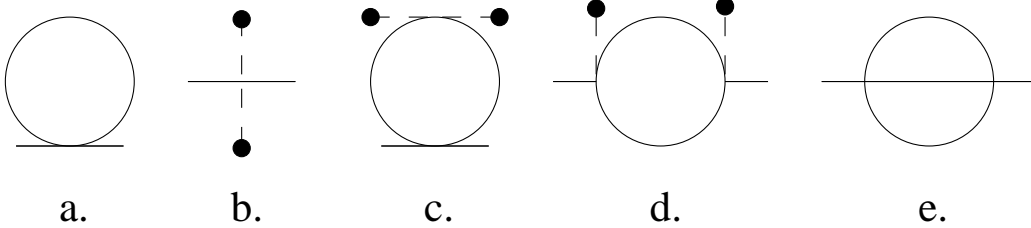


Figure 6: Contributions to the self-energy Π up to $\mathcal{O}(\lambda^2)$.

In the retarded Green function the disconnected piece drops out.

As usual the connected piece satisfies a Dyson-Schwinger equation,

$$D_\Lambda^c(x_1, x_2) = G_\Lambda(x_1 - x_2) + \int dy_1 dy_2 G_\Lambda(x_1 - y_1) \Pi(y_1 - y_2) D_\Lambda^c(y_2, x_2) . \quad (69)$$

The contributions to the self-energy are shown in Fig. 6 up to order λ^2 . To leading order the self-energy is local. The contribution Fig. 6a is removed by a mass counter term and Fig. 6b is the interaction with the background field,

$$\Pi^{(1)}(y_1, y_2) = -i\lambda \phi_\Lambda^2(y_1) \delta(y_1 - y_2) . \quad (70)$$

The free propagator G_Λ may also be split into two contributions which describe propagation forward and backward in time, respectively,

$$G_\Lambda(x_1 - x_2) = G_\Lambda^>(x_1 - x_2) \Theta(t_1 - t_2) + G_\Lambda^<(x_1 - x_2) \Theta(t_2 - t_1) . \quad (71)$$

From Eq. (20) and (30) one reads off,

$$\begin{aligned} G_\Lambda^>(x_1 - x_2) &= \int_{\mathbf{k}} e^{-ik \cdot (x_1 - x_2)} + G_{T,\Lambda}(x_1 - x_2) \\ G_\Lambda^<(x_1 - x_2) &= \int_{\mathbf{k}} e^{ik \cdot (x_1 - x_2)} + G_{T,\Lambda}(x_1 - x_2) . \end{aligned} \quad (72)$$

The corresponding retarded Green function reads

$$\begin{aligned} D_\Lambda^R(x_1 - x_2) &= -i (G_\Lambda^>(x_1 - x_2) - G_\Lambda^<(x_1 - x_2)) \Theta(t_1 - t_2) \\ &= -2 \int_{\mathbf{k}} e^{ik \cdot (x_1 - x_2)} \sin(\omega_{\mathbf{k}}(t_1 - t_2)) \Theta(t_1 - t_2) . \end{aligned} \quad (73)$$

Inserting Eqs. (66) and (71) in the Dyson-Schwinger equation (69) one obtains two coupled integral equations for $D_\Lambda^>(x_1, x_2)$ and $D_\Lambda^<(x_1, x_2)$. For the retarded Green function D_R one finds,

$$D_\Lambda^R(x_1 - x_2) = G_R(x_1 - x_2) + \frac{1}{2}\lambda \int dy G_R(x_1 - y)\phi_\Lambda^2(y)D_\Lambda^R(y - x_2) . \quad (74)$$

This equation is identical with the equation for the classical retarded Green function H_R obtained in [10]. Instead of the classical field $\phi(y)$ now the expectation value $\phi_\Lambda(y)$ appears.

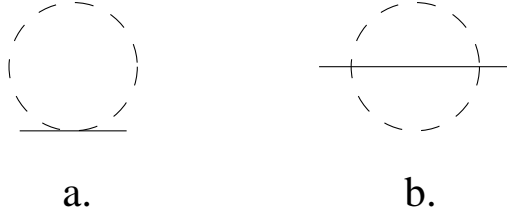


Figure 7: Contributions to the classical self-energy $\bar{\Pi}$ up to $\mathcal{O}(\lambda^2)$.

In order to obtain the complete retarded Green function one has to perform the integration over the soft modes,

$$D_R(x_1, x_2) = \int_{\omega < \Lambda} \mathcal{D}\phi \mathcal{D}\pi e^{-\beta H_\Lambda} D_\Lambda^R(x_1 - x_2) . \quad (75)$$

This means, one has to evaluate the quantities

$$\int_{\omega < \Lambda} \mathcal{D}\phi \mathcal{D}\pi e^{-\beta H_\Lambda} \phi_\Lambda^2(x_1) \dots \phi_\Lambda^2(x_{2n}) . \quad (76)$$

This is completely analogous to the integration over initial conditions in [10]. For two fields one has to leading order in λ (cf. Eq. (37)),

$$\int_{\omega < \Lambda} \mathcal{D}\phi \mathcal{D}\pi e^{-\beta H_\Lambda} \phi_\Lambda(x_1)\phi_\Lambda(x_2) \propto \bar{G}_{T,\Lambda}(x_1 - x_2) . \quad (77)$$

For the products of $2n$ fields one obtains,

$$\begin{aligned} & \int_{\omega < \Lambda} \mathcal{D}\phi \mathcal{D}\pi e^{-\beta H_\Lambda} \phi_\Lambda^2(x_1) \dots \phi_\Lambda^2(x_{2n}) \\ & = 2^n \bar{G}_{T,\Lambda}^2(x_1 - x_2) \dots \bar{G}_{T,\Lambda}^2(x_{2n-1} - x_{2n}) + \text{permutations} . \end{aligned} \quad (78)$$

One easily verifies that the full retarded Green function again satisfies a Dyson-Schwinger equation,

$$D_R(x_1 - x_2) = G_R(x_1 - x_2) + \int dy_1 dy_2 G_R(x_1 - y_1) \bar{\Pi}(y_1, y_2) D_R(y_2, x_2) . \quad (79)$$

The leading contributions to $\bar{\Pi}(y_1, y_2)$ are shown in Fig. 7. The first contribution is subtracted by a mass counter term. The second contribution reads,

$$\bar{\Pi}^{(2)}(y_1, y_2) = \lambda^2 G_R(y_1 - y_2) \bar{G}_{T,\Lambda}^2(y_1 - y_2) . \quad (80)$$

This yields

$$\begin{aligned} \bar{\Pi}^{(2)}(\mathbf{p}, \omega) & = \int dt d^3x e^{i\omega t} e^{-i\vec{p}\vec{x}} \bar{\Pi}^{(2)}(t, \vec{x}) \\ & = \frac{1}{2} \lambda^2 T^2 \sum_{\eta_1, \eta_2, \eta_3} \eta_1 \int_{\omega_1, \omega_2 < \Lambda} d\Phi(\mathbf{p}) \\ & \quad \frac{1}{\omega_2 \omega_3 \omega + \eta_1 \omega_1 + \eta_2 \omega_2 + \eta_3 \omega_3 + i\epsilon} , \end{aligned} \quad (81)$$

where $\eta_i = \pm 1$, $i = 1, \dots, 3$ and

$$d\Phi(\mathbf{p}) = \frac{d^3q_1}{(2\pi)^3 2\omega_1} \frac{d^3q_2}{(2\pi)^3 2\omega_2} \frac{d^3q_3}{(2\pi)^3 2\omega_3} (2\pi)^3 \delta(\mathbf{p} - \mathbf{q}_1 - \mathbf{q}_2 - \mathbf{q}_3) . \quad (82)$$

From Eq. (81) one obtains for the imaginary part of the self-energy ($\omega > 0$),

$$\begin{aligned} \bar{\Gamma}^{(2)}(\mathbf{p}, \omega) & = \frac{\pi}{2} \lambda^2 T^2 \int_{\omega_1, \omega_2 < \Lambda} d\Phi(\mathbf{p}) \frac{1}{\omega_1 \omega_2 \omega_3} [\omega_1 \delta(\omega - \omega_1 - \omega_2 - \omega_3) \\ & \quad + \omega \delta(\omega + \omega_1 - \omega_2 - \omega_3)] . \end{aligned} \quad (83)$$

As discussed in [10], this expression agrees with the imaginary part of the quantum self-energy to order λ^2 for $\omega \ll T$, where the Bose-Einstein distribution function becomes

$$n(\omega) \simeq \frac{T}{\omega} \gg 1 . \quad (84)$$

From Eq. (83) one easily obtains the plasmon damping rate,

$$\gamma = \frac{1}{2m} \Gamma^{(2)}(\mathbf{0}, m) = \frac{1}{1536\pi} \frac{\lambda^2 T^2}{m} \left(1 - \frac{12m}{\pi^2 \Lambda} + \mathcal{O}\left(\left(\frac{m}{\Lambda}\right)^2\right) \right). \quad (85)$$

Except for the corrections $\mathcal{O}\left(\frac{m}{\Lambda}\right)$ the result agrees with the quantum result to leading order in λ [9]. The dependence on the infrared cutoff Λ controls the size of corrections to the infrared limit.

To assess the size of the quantum corrections one has to compute the contribution of Fig. 6d to the damping rate (diagram c. does not contribute to the imaginary part, diagram e. contains less IR dominant propagators and therefore gives a smaller contribution). The correction to the classical self-energy $\bar{\Pi}$ reads (cf. appendix)

$$\delta\bar{\Pi}(y_1, y_2) = \frac{\lambda^2}{2} \bar{G}_{T,\Lambda}^2(y_1 - y_2) \left[G_{++}^2(y_1 - y_2) - G_{+-}^2(y_1 - y_2) \right]. \quad (86)$$

After some algebra one finds for the correction to the imaginary part of the on-shell self-energy ($\mathbf{p} = 0$, $\omega = m$),

$$\begin{aligned} \delta\bar{\Gamma}^{(2)}(\mathbf{0}, m) &= \frac{\lambda^2}{2} \pi T \int d\Phi(\mathbf{0}) \frac{1}{\omega_1} \delta(m + \omega_1 - \omega_2 - \omega_3) \\ &= \frac{\lambda^2 T^2}{768\pi} \cdot \frac{6}{\pi^2} \left(\beta m \ln \frac{m}{2\Lambda} + \mathcal{O}(\beta\Lambda) \right). \end{aligned} \quad (87)$$

At high temperatures $m^2 \sim \lambda T^2$, i.e., the quantum corrections are $\mathcal{O}(\sqrt{\lambda} \ln \lambda)$. This implies that the classical limit gives a meaningful approximation to the quantum theory only to the leading order in λ [10].

6 Summary

We have shown that in scalar quantum field theories at high temperature the behaviour of low frequency modes is described by an effective classical theory. Corrections to this classical limit are controlled by the dependence of observables on an infrared cutoff Λ which is introduced to separate soft modes from hard modes.

Integrating out the hard modes yields an effective theory which depends on the infrared cutoff Λ and on a classical background field $\phi_\Lambda(x)$, the expectation value of the field operator in a coherent state containing soft modes

only. The thermal Green functions of the low energy effective theory factorize in products of expectation values of the field operator up to corrections of order $\hbar\beta\Lambda$. This loss of quantum coherence is due to the interactions with the soft modes in the thermal bath. The behaviour of soft modes is described by classical statistical field theory.

The separation of soft and hard modes has been carried out at some fixed initial time t_i . Due to interactions with the thermal bath soft and hard modes will mix at later times. The implications for the behaviour of correlation functions at large times remain to be studied.

Our analysis also illustrates some of the difficulties which have to be faced in calculations of real-time correlation functions in gauge theories at high temperature. The separation of soft and hard thermal modes is complicated by gauge invariance and in the cases of interest the gauge coupling is rather large, so that the magnetic mass scale g^2T is not well separated from the temperature T . Hence, it is not clear to us how accurately existing classical numerical simulations for real-time correlation functions in gauge theories approximate the quantum theory.

We would like to thank D. Boyanovsky, M. Lüscher, A. Patkós and J. Polónyi for helpful discussions and comments. This work has been partially supported by the Hungarian NSF under contract OTKA-T22929.

Appendix

The contour integral in Eq. (61) is most easily evaluated in the two-component formalism which is obtained by taking the limits $t_i \rightarrow -\infty$, $t_f \rightarrow \infty$. Then only the contributions from the parts C_+ and C_- of the Keldysh-type contour in Fig. 1 remain.

The corresponding propagators read (cf. [16])

$$\begin{aligned} G_{++}(x_1 - x_2) &= \Theta(t_1 - t_2)G^>(x_1 - x_2) + \Theta(t_2 - t_1)G^<(x_1 - x_2) \\ &= (G_{--}(x_1 - x_2))^* , \end{aligned} \tag{88}$$

$$G_{+-}(x_1 - x_2) = G^<(x_1 - x_2) = (G_{-+}(x_1 - x_2))^* , \tag{89}$$

where

$$G^{>(<)}(x) = \int_{\mathbf{k}} G^{>(<)}(\mathbf{k}, t) e^{i\mathbf{k}\mathbf{x}} , \tag{90}$$

$$\begin{aligned}
G^>(\mathbf{k}, t) &= e^{-i\omega_{\mathbf{k}}t} + 2\frac{n(\omega_{\mathbf{k}})}{\omega_{\mathbf{k}}} \cos \omega_{\mathbf{k}}t \\
&= (G^<(\mathbf{k}, t))^* .
\end{aligned} \tag{91}$$

The interactions of the two fields ϕ_+ and ϕ_- which correspond to the two branches C_+ and C_- , respectively, are given by

$$\begin{aligned}
S_I &= - \int dt \int d^3x \frac{\lambda}{4!} \left((\phi_+ + \phi_\Lambda)^4 - (\phi_- + \phi_\Lambda)^4 \right) \\
&= - \int dt \int d^3x \lambda \left(\frac{1}{6}(\phi_+ - \phi_-)\phi_\Lambda^3 + \frac{1}{4}(\phi_+^2 - \phi_-^2)\phi_\Lambda^2 \right. \\
&\quad \left. + \frac{1}{6}(\phi_+^3 - \phi_-^3)\phi_\Lambda + \frac{1}{24}(\phi_+^4 - \phi_-^4) \right) ,
\end{aligned} \tag{92}$$

where ϕ_Λ is the background field introduced in Sect. 2.

For the contribution of diagramm 5i one now obtains

$$\begin{aligned}
&\frac{\lambda^2}{4} \phi_\Lambda(x) \int_c dx' G_\Lambda(x, x')^2 \hat{\Phi}(x')_\Lambda^2 \\
&= \frac{\lambda^2}{4} \phi_\Lambda(x) \int d^4x' \left(G_{++}(x - x')^2 - G_{+-}(x - x')^2 \right) \phi_\Lambda^2(x') \\
&= \frac{\lambda^2}{4} \phi_\Lambda(x) \int dt' \Theta(t - t') \int d^3x' \left(G^>(x - x')^2 - G^<(x - x')^2 \right) \phi_\Lambda^2(x') .
\end{aligned}$$

Inserting the expressions for the propagators $G^>$ and $G^<$ and performing a partial integration with respect to t' one obtains the result Eq. (64).

References

- [1] For a discussion and references, see
V. A. Rubakov and M. E. Shaposhnikov, *Usp. Fiz. Nauk.* **166** (1996) 493
- [2] D. Yu. Grigoriev and V. A. Rubakov, *Nucl. Phys.* **B229** (1988) 67
- [3] J. Ambjørn and A. Krasnitz, *Phys. Lett.* **B362** (1995) 97; preprint NBI-HE-97-18, hep-ph/9705380
- [4] P. Arnold, D. Son and L. Yaffe, *Phys. Rev.* **D55** (1997) 6264
- [5] G. Parisi, *Statistical Field Theory* (Addison-Wesley, New York, 1988)
- [6] D. Bödeker, L. McLerran and A. Smilga, *Phys. Rev.* **D52** (1995) 4675
- [7] D. Bödeker, *Nucl. Phys.* **B486** (1997) 500
- [8] R. R. Parwani, *Phys. Rev.* **D45** (1992) 4695; *ibid.* **D48** (1993) 5965 (E);
E. Wang and U. Heinz, *Phys. Rev.* **D53** (1996) 899
- [9] G. Aarts and J. Smit, *Phys. Lett.* **B393** (1997) 395; preprint THU-97-15,
hep-ph/9707342
- [10] W. Buchmüller and A. Jakovác, *Phys. Lett.* **B407** (1997) 39
- [11] A. Jakovác, *Classical Limit in Scalar QFT at High Temperature*, in
Proc. of *Strong and Electroweak Matter '97* (Eger, Hungary, May 1997),
to appear; DESY 97-148, hep-ph/9708229
- [12] B. J. Nauta and Ch. G. van Weert, hep-ph/9709401
- [13] L. D. Landau and E. M. Lifshitz, *Statistical Physics* (Pergamon Press,
London, 1959)
- [14] N. Tetradis and C. Wetterich, *Nucl. Phys.* **B398** (1993) 659
- [15] M. D'Attanasio and M. Pietroni, *Nucl. Phys.* **B472** (1996) 711
- [16] N. P. Landsman and Ch. G. van Weert, *Phys. Rep.* **145** (1987) 141

- [17] C. Itzykson and J.-B. Zuber, *Quantum Field Theory* (McGraw-Hill, New York, 1980)
- [18] A. J. Niemi and G. W. Semenoff, *Ann. of Phys.* **152** (1984) 105
- [19] J. Zinn-Justin, *Quantum Field Theory and Critical Phenomena* (Clarendon Press, Oxford, 1993)
- [20] D. Boyanovsky, H. J. de Vega, R. Holman, D.-S. Lee and A. Singh, *Phys. Rev.* **D51** (1995) 4419
- [21] A. Jakovác, *Phys. Rev.* **D53** (1996) 4538;
A. Jakovác and A. Patkós, *Nucl. Phys.* **B494** (1997) 54